NEW INTERFACE ELEMENT WITH NON-COINCIDENT NODES TO SIMULATE DISCRETE DAMAGE IN COMPOSITE LAMINATE

A. Trellu[1,2], C. Bouvet[1], S. Rivallant[1] and L. Ratsifandrihana[2]

[1]Université de Toulouse, ISAE-SUPAERO, Institut Clément Ader (UMR CNRS 5312)
10 av. E. Belin, 31055 Toulouse, FRANCE
Email: antoine.trellu@isae.fr, christophe.bouvet@isae.fr, samuel.rivallant@isae.fr
[2]SEGULA Aerospace and Defence
24 bd. Déodat de Severac, 31770 Colomiers, FRANCE
Email: leon.rastifrandrihana@segula.fr

Keywords: Crack propagation, Interface element, DCB, Impact, Modeling and simulation

Abstract
Composite failure phenomena remain complex and lead to over-sizing structures in many industries involving long and costly experimental campaigns. Numerical approaches are good alternative to decrease sizing costs. The Discrete Ply Model developed in Institut Clément Ader over these last 10 years shows good results in simulations of impact and compression after impact of laminates, ply drop-offs, open hole tensile tests… But the present approach leads to certain limitations for complex draping sequences. A new interface element is implemented in the model to fix these limitations. The present paper details the first step of the new interface element implementation and validation, then its improvement is discussed.

1. Introduction

1.1. Context

Because of their high strength-to-weight ratio, composites are more and more used for manufacture of aeronautical, railway and automotive structures. However, their vulnerability to out of plane stresses, leads to an over-sizing. These stresses, as low velocity impact, involve complex failure phenomena and lead to a significant reduction of the residual properties. To decrease structures sizing costs, models are developed to simulate composite's mechanical behavior and the different failures appearing in composite structure [1, 2]. Since the 90's many works deal with the simulation of the failures induced by low velocity impacts [3-6].

It is the case of the "Discrete Ply Model" (DPM), developed by Bouvet et al. for over 10 years [7-9]. This model allows the representation of the three main failures appearing in a composite structure, which are: matrix cracking, delamination and fiber failure.

1.2. The DPM

This part is just a brief recall of the main ideas done by the DPM. Interested reader can find more details of the model in [9]. The following figure (Fig. 1) presents the concept of the DPM:

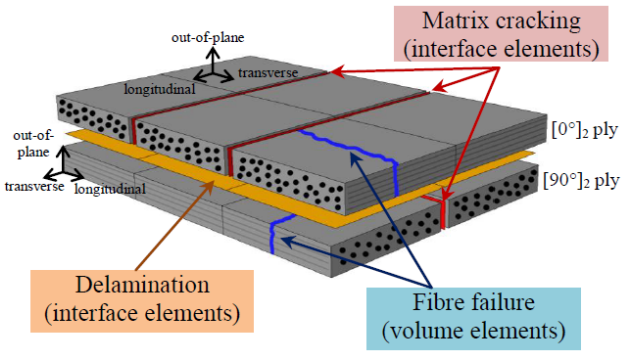

Figure 1. DPM concept [9]

- Delamination is simulated with interface elements between two consecutive plies (each ply is modeled with one volume finite element in the thickness). The four upper nodes of the bottom ply and the four lower nodes of the top ply are coincident and form the zero thickness interface element. Interface damage is driven using fracture mechanics calculated with an equivalent displacement (Eq. 3) :

$$d_{eq} = \sqrt{(\langle d_I \rangle^+)^2 + \left(\frac{d_I^0}{d_{II}^0} d_{II}\right)^2 + \left(\frac{d_I^0}{d_{III}^0} d_{III}\right)^2} \quad (1)$$

Where d_I^0, d_{II}^0 et d_{III}^0 are the critical displacements for damage initiation, respectively in fracture mode *I*, *II* and *III*. Once damage initiation displacement d_{eq} is reached, damage propagation is done by a linear or exponential law to release stresses and dissipate the energy release rate. In the DPM, the delamination in mode *II* and *III* are considered equal.

- Matrix cracking is modeled with interface elements located between volume elements in the ply direction. This damage is driven using Hashin's criterion (Eq. 2) calculated in neighboring volume elements.

$$\left(\frac{\sigma_t^+}{\sigma_t^f}\right)^2 + \frac{\tau_{lt}^2 + \tau_{tz}^2}{\left(\tau_{lt}^f\right)^2} \leq 1 \quad (2)$$

With σ_t^+ the positive value of the transverse stress, σ_t^f the transverse failure stress, τ_{lt} and τ_{tz} the shear stresses, and τ_{lt}^f the shear failure stress. When the criterion is reached, element stiffness is set to zero, and the two volume elements become independent. Even if the matrix cracking is not detrimental for the global failure of the ply, it is very significant because delamination is usually linked to it [10, 11].

- Fiber failure is taken into account using conventional continuum damage and failure mechanics. When damage initiation strain ε_0^t in traction or ε_0^c in compression is reached, a damage variable corresponding to a linear decrease of the stress until the final damage strain ε^1 is calculated and stresses are determined from the damaged stiffness matrix.

ε^1 is calculated to ensure that the fiber energy release rate in mode *I*, $G_I^{f,t}$ in traction or $G_I^{f,c}$ in compression, is dissipated. The following equation (Eq. 1) describes the fiber failure criterion.

$$\int_V \left(\int_0^{\varepsilon^1} \sigma_l d\varepsilon_l \right) . dV = S . G_I^f \tag{3}$$

Where V and S are the volume and the section of the element and σ_l and ε_l the longitudinal stress and strain.

The DPM presents two major advantages. The first one is the good representation of discrete damages taking into account the coupling of the different failure modes. The second one is the use of a low number of material parameters with physical meaning: elastic properties, failure limits and critical energy release rates for each failure mode.

However, the present approach leads to certain limitations. To have a good representation of the matrix cracking, volume elements are oriented in the fiber directions. Since current delamination interface elements have coincident nodes with volume elements of the neighboring plies, only standard ply orientations (0°, 90° and ±45°) can be used, and the size of element in the different plies are linked. It can also induces high computation times.

In order to fix these issues, a new interface element is developed in Abaqus, using a VUEL subroutine and implemented in the model. First, this paper presents the element principle and formulation and, secondly, the first results obtained with the new element.

2. New interface element formulation

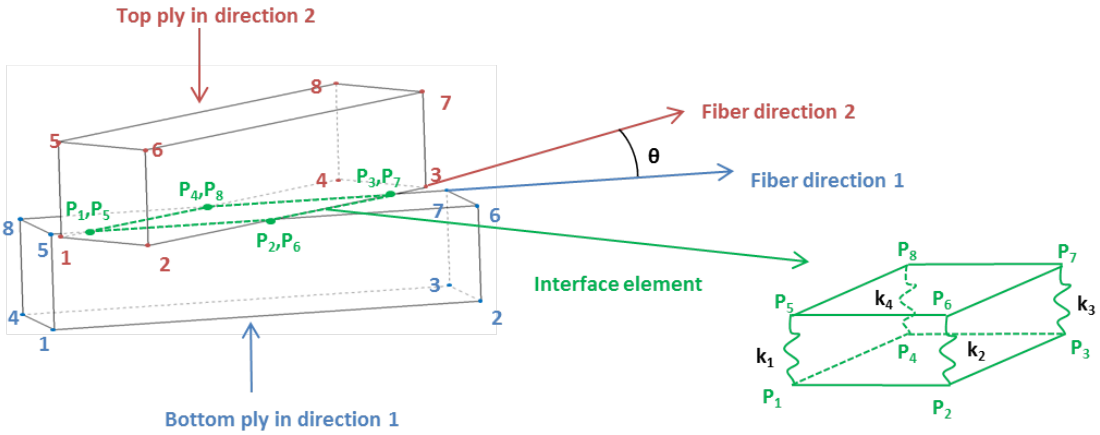

Figure 2. New interface element

The above figure (Fig.2) presents the new delamination interface element between two volume elements with different fiber orientation. It is defined by the four upper nodes of the bottom ply (5, 6, 7 and 8 in blue) and the four lower nodes of the top ply (1, 2, 3 and 4 in red). Of course these nodes are not coincident. The real interface element is represented by the nodes P_1 to P_8 (in green) and corresponds to the intersection area between the two volume elements. This interface is showed in three dimensions in the figure for a better understanding but at the initial state, it is a zero thickness element. The finite element calculation aim is to determine the forces at nodes 1 to 8, taking account of eventual failure propagation in the element.

The real interface is modeled with four springs with k_1, k_2, k_3 and k_4 as stiffness coefficients. Displacements at nodes P_1 to P_8 are determined according to displacements of the volume elements nodes and through a shape functions matrix. This matrix is composed by distance ratios λ_1 to λ_8 which are calculated at the initial state (Fig. 3).

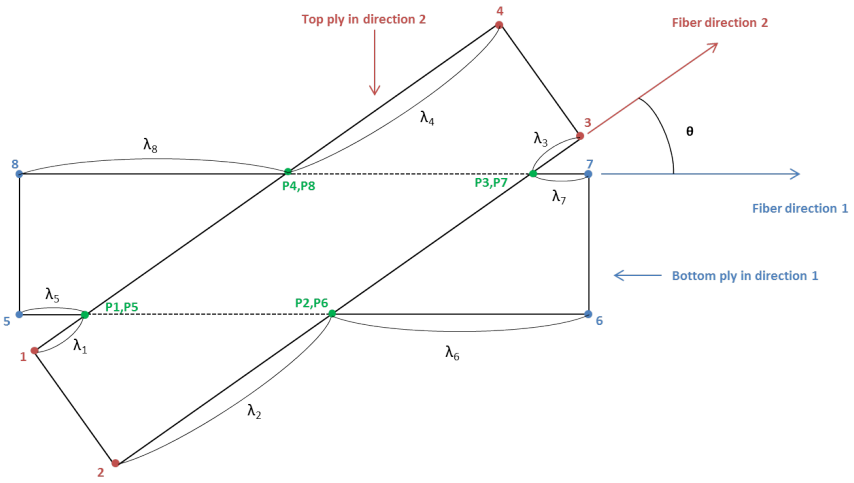

Figure 3. Distance ratios $\boldsymbol{\lambda_1}$ to $\boldsymbol{\lambda_8}$

Following equations (Eq. 4 and Eq. 5) give displacement calculation for nodes P_1 to P_8 according to volume elements nodes displacements U_1 to U_8 and the shape functions matrix $\underline{\underline{\pi}}$.

$$\begin{bmatrix} U_{P1} \\ \vdots \\ U_{P8} \end{bmatrix} = \underline{\underline{\pi}} \begin{bmatrix} U_1 \\ \vdots \\ U_8 \end{bmatrix} \tag{4}$$

$$\underline{\underline{\pi}} = \begin{pmatrix} 0 & 0 & 0 & 0 & 1-\lambda_5 & \lambda_5 & 0 & 0 \\ 0 & 0 & 0 & 0 & \lambda_6 & 1-\lambda_6 & 0 & 0 \\ 0 & 0 & 0 & 0 & 0 & 0 & 1-\lambda_7 & \lambda_7 \\ 0 & 0 & 0 & 0 & 0 & 0 & \lambda_8 & 1-\lambda_8 \\ 1-\lambda_1 & 0 & 0 & \lambda_1 & 0 & 0 & 0 & 0 \\ 0 & 1-\lambda_2 & \lambda_2 & 0 & 0 & 0 & 0 & 0 \\ 0 & \lambda_3 & 1-\lambda_3 & 0 & 0 & 0 & 0 & 0 \\ \lambda_4 & 0 & 0 & 1-\lambda_4 & 0 & 0 & 0 & 0 \end{pmatrix} \tag{5}$$

The element stiffness matrix $\underline{\underline{K}}$ is calculated with the four spring stiffness coefficients and allows to determine forces at nodes P_1 to P_8 according to the displacements U_{P1} to U_{P8} (Eq. 6 and Eq. 7).

$$\begin{bmatrix} F_{P1} \\ \vdots \\ F_{P8} \end{bmatrix} = \underline{\underline{K}} \begin{bmatrix} U_{P1} \\ \vdots \\ U_{P8} \end{bmatrix} \tag{6}$$

$$\underline{\underline{K}} = \begin{pmatrix} k1 & 0 & 0 & 0 & -k1 & 0 & 0 & 0 \\ 0 & k2 & 0 & 0 & 0 & -k2 & 0 & 0 \\ 0 & 0 & k3 & 0 & 0 & 0 & -k3 & 0 \\ 0 & 0 & 0 & k4 & 0 & 0 & 0 & -k4 \\ -k1 & 0 & 0 & 0 & k1 & 0 & 0 & 0 \\ 0 & -k2 & 0 & 0 & 0 & k2 & 0 & 0 \\ 0 & 0 & -k3 & 0 & 0 & 0 & k3 & 0 \\ 0 & 0 & 0 & -k4 & 0 & 0 & 0 & k4 \end{pmatrix} \tag{7}$$

Then the delamination law presented in the introduction (Eq. 3) is used. When the equivalent displacement d_{eq} is reached for one of the springs, stiffness coefficient of the considered spring is decreased until the good energy release rate is dissipated. Then forces at nodes 1 to 8 of the interface element are calculated with the following relation (Eq. 8):

$$\begin{bmatrix} F_{P1} \\ \vdots \\ F_{P8} \end{bmatrix} = \underline{\underline{\pi}}^t \underline{\underline{K}} \underline{\underline{\pi}} \begin{bmatrix} U_1 \\ \vdots \\ U_8 \end{bmatrix} \tag{8}$$

Where $\underline{\underline{\pi}}^t$ is the transposed shape functions matrix.

3. First results

To validate this new interface element, a « Double Cantilever Beam » (DCB) test is simulated, allowing to test interface elements in fracture mode *I*. In the model, the crack is initiated with a zone without interface elements. The Table 1, gives T700/M21 properties, the material used to run simulations.

Table 1. T700/M21 mechanical properties

E_l^t (GPa)	E_l^c (GPa)	E_t (GPa)	ν_{lt}	G_{lt} (GPa)	G_{lz} (GPa)
130	100	7.7	0.3	4.75	2.9
σ_t^f (MPa)	σ_c^f (GPa)	σ^{crush} (MPa)	ε_t^0	ε_c^0	
60	110	250	0.018	-0.0125	
G_{Ic}^d (N/mm)	G_{IIc}^d (N/mm)	G_t^f (N/mm)	G_c^f (N/mm)		
0.4	1.8	130	40		

The stacking sequence is $[0°_2/90°/0°_2]$ (the red colored line in the draping sequence indicates the delaminated interface), and ply thickness is 0.25 mm. The schema of the following figure (Fig. 4) shows test characteristics and specimen dimensions. Specimen width is 2 mm. F is the force applied to propagate the damage and δ is the respective opening.

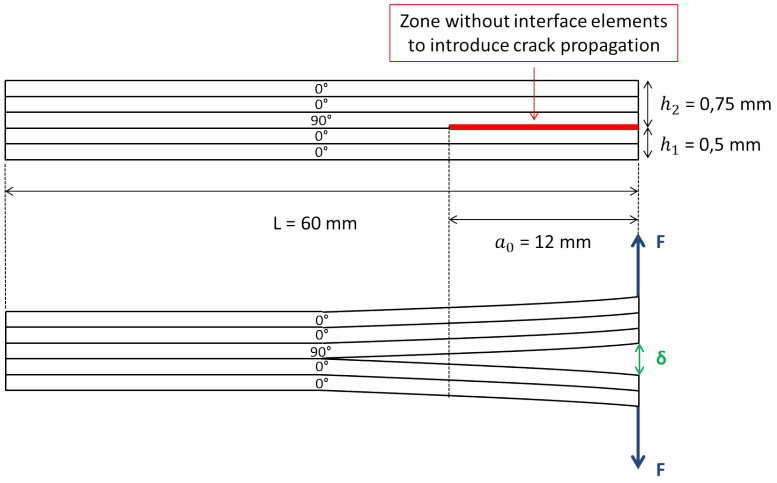

Figure 4. DCB specimen

Several numerical simulations are launched. First, for purposes of comparison, a DCB test with Abaqus interface elements is done, nodes are coincident and element size is 0.5 x 0.5 mm^2 (Fig. 5-a). Volume elements are meshed with C3D8I elements because of their good bending behavior.

This test is run with COH3D8 interface elements and the DPM delamination law. This simulation is used as reference. Different configurations of the DCB test with new interface elements are simulated by changing element length in the fiber direction and maintaining the distance between two matrix cracking interfaces (Fig. 5-b, 5-c). The final objective is to increase the length to width ratio by five.

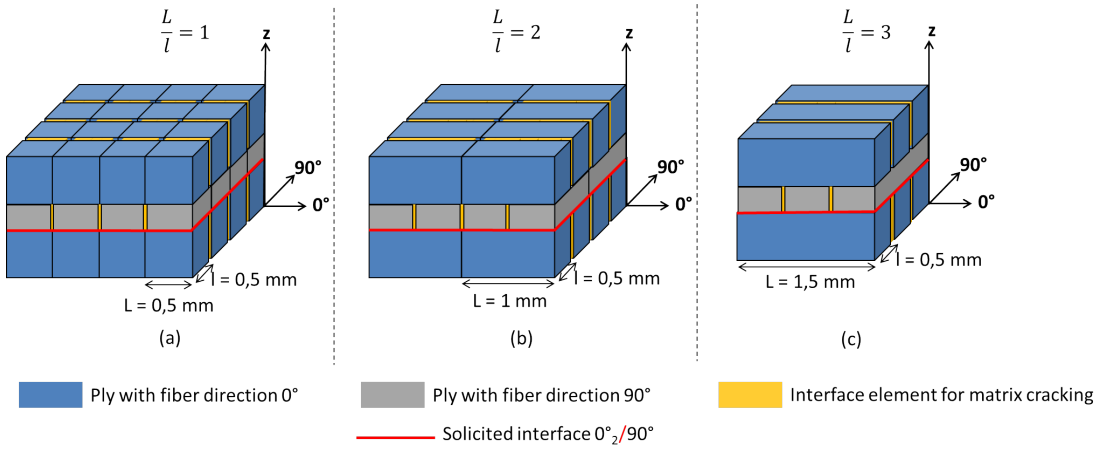

Figure 5. Different mesh configurations tested

Figure 6 shows crack propagation (seen from above) for different configurations tested where the opening displacement, δ, is 3.5 mm. If the damage value is one, the element is totally delaminated.

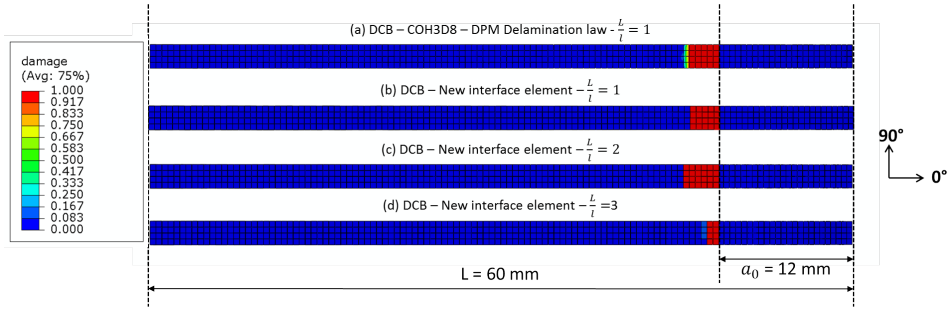

Figure 6. Crack propagation for 3.5 mm opening displacement

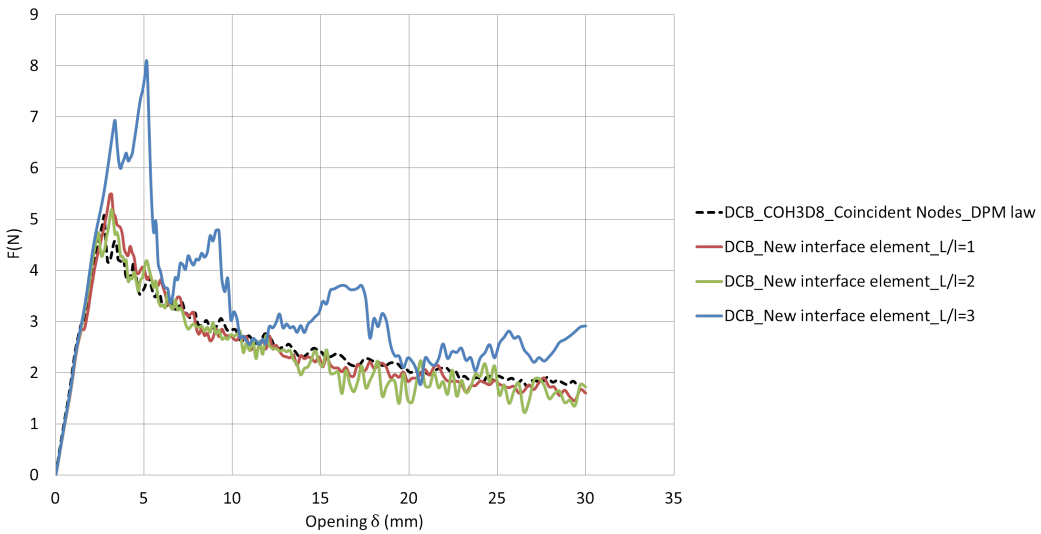

Figure 7. Curve of the force according to the opening displacement

Curves obtained with the new interface element for $\frac{L}{l} = 1$ and $\frac{L}{l} = 2$, show a good correlation with the DPM reference case (Fig. 6-a, 6-b, 6-c, 7). When the length to width ratio exceeds two, some instabilities appear and perturb the crack propagation (Fig. 6-d, 7).

In fact, when volume element length is increased, bending behavior is not properly represented. Element curvature is nearly not taken into account when element length to width ratio is greater than 2 (Fig. 8). This issue involves a rough crack propagation and delamination area on the above interface 90°/0°, which explain curve instability for $\frac{L}{l} = 3$.

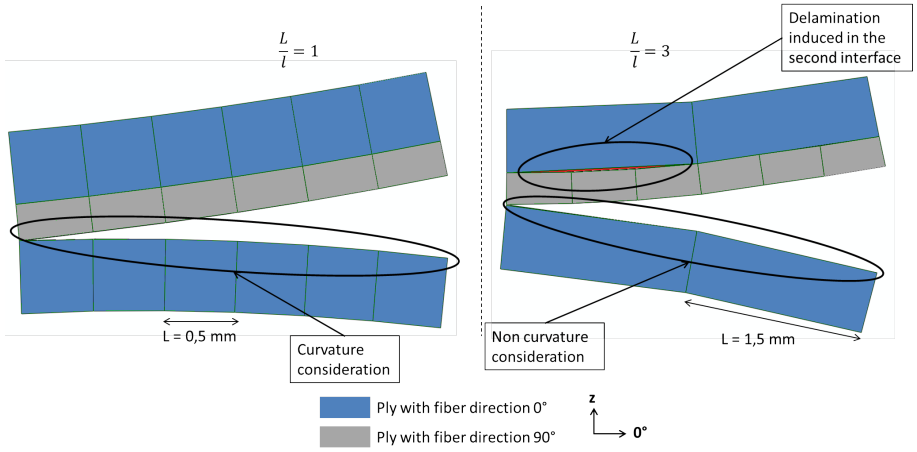

Figure 8. Bending behavior issue

In order to fix this problem, the curvature in interface elements is now implemented in the interface element formulation. A new shape function, allows to adjust P_1 to P_8 position in z-direction to take into account the element curvature (Fig. 9). The curvature of the interface element is now defined with the new position point P'_1 to P'_8. For example, P'_{31} is the new P_1 position of the third interface element.

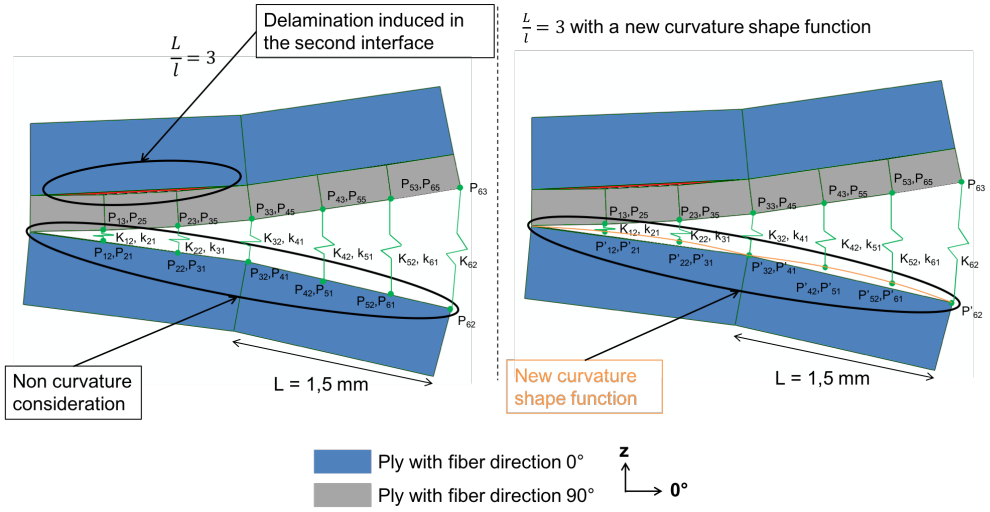

Figure 9. New curvature shape function

Conclusion

A new interface element was developed to use delamination interface elements with non-coincident nodes, allowing to use unusual stacking sequences, to change the distance between matrix cracking interface in two consecutive plies and to reduce elements number. New interface element behavior is validated in fracture mode *I* until $\frac{L}{l} = 2$. When the element length to width ratio in the fiber direction exceeds 2 mm, bending behavior is not accurately taken into account. This work is currently in progress. This new element must also be tested in mode *II* with ENF tests. Then impact simulations will be run to conclude on the decrease of calculation time involved by this new interface element.

References

[1] Wisnom M.R. Modelling discrete failures in composites with interface elements. *Composites Part A:Applied Science and Manufacturing,* 41(7):795-805, 2010.

[2] Silberschmidt V. *Dynamic deformation, damage and fracture in composite materials and structures*. Woodhead Publishing, Elsevier, 2016.

[3] S. Abrate. *Impact on Composites Structures*. Cambridge University Press, 1998

[4] O. Eve. Etude du comportement des structures composites endommagées par impact basse vitesse. PhD Thesis, University of Metz, France, 1999.

[5] M.O.W. Richardson, M.J. Wisheart. Review of low-velocity impact properties of composite materials. *Composites Part A:Applied Science and Manufacturing*, 27(12):1123-1131, 1996.

[6] W.J. Cantwell, J. Morton. The impact resistance of composite materials – a review. *Composites*, 22(5):347-362, 1991.

[7] Bouvet C., Castanié B., Bizeul M., Barrau J.J. Low velocity impact modeling in laminate composite panels with discrete interface elements. *International Journal of Solids and Structures*, 46(14-15):2809-21, 2009.

[8] Bouvet C., Rivallant S., Barrau J.J. Low velocity impact modeling in composite laminates capturing permanent indentation, *Composite Science and Technology*, 72:1977-88, 2012.

[9] Hongkarnjanakul N., Bouvet C., Rivallant S. Validation of low velocity impact modelling on different stacking sequences of CFRP laminates and influence of fibre failure, *Composite Structures*, 106:549-59, 2013.

[10] M.F.S.F de Moura, J.P.M. Gonçalves. Modelling the interaction between matrix cracking and delamination in carbon–epoxy laminates under low velocity impact. *Composites Science and Technology* 64:1021-1027, 2004.

[11] S. R. Hallett, W.G. Jiang, B. Khan, M.R. Wisnom. Modelling the interaction between matrix cracks and delamination damage in scaled quasi-isotropic specimens. *Composites Science and Technology* 68(1):80-89, 2008.